Abstract We present an overview of the optical properties of nonlinear surface plasmon polaritonic crystals and their applications to control light with light. Surface plasmon polaritonic crystals are periodically nanostructured metal surfaces or thin metal films that act as two-dimensional photonic crystals for surface polaritons. Hybritization of such nanostructures with dielectrics exhibiting an optical nonlinear response allows utilization of the electromagnetic field enhancement effects to observe nonlinear effects and bistable behaviour at low light intensities. By changing the geometry of the nanostructured film, the dispersion of the crystal is modified and, thus, electromagnetic mode structure and associated density of states can be controllably tuned in the desired spectral range. This provides enhanced flexibility in engineering the nonlinear optical response of plasmonic crystals in a chosen spectral range for both control and signal wavelengths.

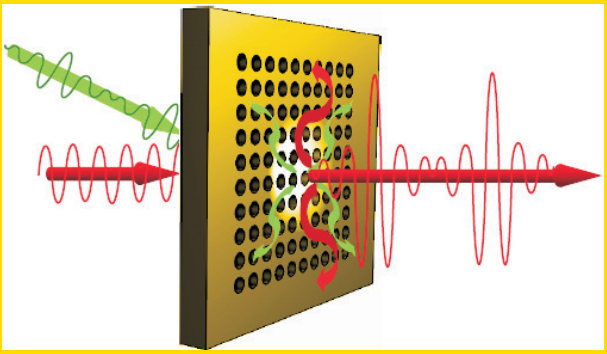

Schematics of the interaction of a control beam (green) and a signal beam (red) via surface plasmons on a gold film with nonlinear plasmonic crystal.

Nonlinear surface plasmon polaritonic crystals

Gregory A. Wurtz and Anatoly V. Zayats[*]

Centre for Nanostructured Media, IRCEP, The Queen's University of Belfast, Belfast BT7 1NN, United Kingdom

Received: 26 February 2008, Revised: 14 March 2008, Accepted: 17 March 2008
Published online: 23 April 2008

Key words: Surface plasmons; metallic nanostructures; Kerr nonlinearity; all-optical switching; optical bistability

PACS: 42.65.Pc, 73.20.Mf, 78.20.-e

1. Introduction

All-optical signal processing in integrated photonic circuits and its applications in optical communications and computing require the ability to control light with light [1, 2]. Nonlinear optical effects needed for this purpose can be achieved with slow molecular motion nonlinearities (ms timescales), such as in liquid crystals [3, 4], or ultra-fast electronic nonlinearities (up to fs timescales) [5]. All-optical devices based on various types of optical nonlinearities have been considered in the past. The main drawbacks of the majority of such devices are twofold. First, the limitation on their minimum size required to provide a sufficient light passlength to achieve a sizeable nonlinear response and, second, the relatively high operational light intensities. To remediate to these limitations, very recently, nonlinear optical devices based on photonic crystal defects have been proposed that utilize the electromagnetic field confinement and enhancement at the photonic defect location to enhance nonlinear effects [2, 6–8].

However, stronger field enhancements can be achieved using plasmonic nanostructures to tailor electromagnetic modes with effective size well below the diffraction limit of the light. A significant field enhancement is routinely obtained in plasmonic devices in various arrangements for surface enhanced Raman scattering, stimulated emission, second-harmonic generation and photon tunnelling [9, 10]. This enhancement is the result of the increased density of electromagnetic states near a metal surface corresponding to the spectrum of plasmonic excitations. Coupling a control light to such surface electromagnetic modes is, therefore, a possible way to enhance the effective nonlinearity of the hybrid nanostructures formed when a nonlinear material is placed near the metal surface [11].

One of the examples of such nonlinear optical metamaterials are bulk nonlinear materials doped with metallic nanoparticles [12–14]. In such metamaterials, the excitation of the hybrid structure at the wavelengths of the localised surface plasmon resonances of the nanoparticles leads to

Corresponding author: e-mail: a.zayats@qub.ac.uk

an increase in the effective nonlinear susceptibility of the composite material compared to either materials taken separately. Similarly, the coverage of metallic nanoparticle arrays, e.g., nanospheres or nanorod assemblies, with nonlinear material results in the enhancement of the nonlinear response of the dielectric while also lowering the light intensities required for nonlinear action [15, 16]. The utilisation of the field enhancement effects associated with localised surface plasmons modes has also been shown to enable controlled photon tunneling through nanoscale pinholes in a metal film covered with nonlinear polymer [17, 18]. In particular, measurements of photon tunneling through individual, naturally occurring, nanometer scale pinholes have provided indication of "photon blockade" effects, similar to Coulomb blockade phenomena observed in single-electron tunneling experiments [17]. The observations of photon tunneling being gated by light at a different wavelength have also been reported with similar but somewhat larger pinholes [18].

Concurrently, if surface plasmons in the form of surface plasmon polaritons (propagating surface waves) are chosen to be a signal carrier, the strong sensitivity of their resonances to the structured surface where they propagate [9,19] could bring a viable solution to the problem of their all-optical control. In this scheme, minute changes induced in the refractive index of a nonlinear material placed on the metal surface would significantly influence the surface plasmon resonant conditions and surface polariton propagation along the surface. This was first shown with smooth metal films in the Kretschmann geometry using liquid crystal phase transformations under the influence of thermal effects of light. Both switching of the reflected light and bistability with the variation of the intensity of the incident light was observed [3]. The latter was explained by a positive feedback due to the intensity dependent refractive index of the liquid crystal placed on the metal film and illuminated by the evanescent field of the surface plasmon polariton (SPP) wave. Nanostructured metal surfaces such as surface plasmon polaritonic crystals (SPPCs) [9, 20–23] provide much more flexibility for tailoring the wavelength-dependent resonant conditions and the electromagnetic field enhancement conditions in a few-wavelength-size devices. Thus, integratable all-optical devices can be developed using nonlinear surface plasmon polaritonic crystals.

SPP crystals have optical properties similar to two-dimensional photonic crystals but act on surface polaritons rather than "bulk" photons. SPPCs are most often considered with either a periodic arrangement of groves or stripes (1D SPPC) or as a two-dimensional periodic arrangement of holes or bumps of various shapes (2D SPPC). A fundamental difference between conventional photonic and surface polaritonic crystals comes from a different electromagnetic field distribution close to the surface. Surface polaritons are intrinsically two-dimensional excitations whose electromagnetic field is concentrated at a metal-dielectric interface. Thus, in contrast to photonic crystals, strong electromagnetic field enhancement takes place at a SPP crystal's interface related to the surface polariton's field confinement [24]. This enhancement results in a much stronger effective nonlinear optical response achievable with surface polaritonic crystals as it is related to the local field strength [25, 26]. This can significantly assist nonlinear optical mixing in such structures. The advantage of a surface polaritonic crystal for the development of all-optical active elements is two-fold: a high sensitivity of SPP resonances to minor modifications of optical properties of surroundings, and the electromagnetic field enhancement related to surface plasmon modes that can allow achieving these modifications via the optical Kerr effect at low illuminating light intensities. As a consequence of dielectric constant change, the SPP modes will experience a frequency shift, thus modifying the resonant conditions of the SPP mode excitation and related optical transmission or reflection.

Although optical nonlinearities from the metal itself were considered in SPPC [27, 28], the stronger nonlinear response can be observed if an SPP crystal is hybridized with a nonlinear material. Nonlinear SPP crystals simultaneously take advantage of both the field enhancement at the control light frequency and the sensitivity of SPPs at the signal light frequency to the permittivity changes induced by the control light. These properties have been utilised to demonstrate light control with light and its bistable behaviour in nonlinear SPPCs [25, 26]. Theories of nonlinear effects were developed considering bare as well as hybridized SPP crystals [27, 29, 30]. In both configurations, bistability in the optical transmission of the SPP crystals was predicted.

In the following, we overview the results on nonlinear transmission of light through surface polaritonic crystals, transmission bistability effects and related modulation of light by light that becomes possible due to coupling to the Bloch modes of SPPCs. Finally, optical self-limiting effects in the transmission through defects in SPPCs will be considered.

2. Nonlinear transmission of surface polaritonic crystals

Nonlinear optical transmission through hybridised plasmonic structures can be observed in a variety of geometries. Two main configurations can be considered where self-induced effects of the light interacting with plasmonic excitations in a nonlinear environment occur or external-light-controlled nonlinear effects trigger the nonlinear behaviour of the crystal. In general, nonlinear effects are observed in all transmission resonances related to SPP Bloch wave excitations [26], cylindrical surface plasmons [25], as well as localised surface plasmons at individual defects in the metal films [17, 18]. However, since the field enhancement effect depends on the SPP crystal parameters as well as on the localised surface plasmon modes supported by the nanostructure, the range of the control light intensities depends on the geometrical and material properties of the nanostructures and is, therefore, a complex function of the crystal under consideration.

To identify the general mechanisms of the nonlinear transmission, let us consider the optical transmission through periodic arrays of holes in a metal film. These structures support plasmonic excitations consisting of the SPP Bloch modes related to the periodic modulation of the metal-dielectric interface convoluted with localised plasmonic and/or waveguided modes of the holes. The latter contribution reflects the geometry of the holes, i.e. the hole size, shape, and film thickness, and can be either strongly or weakly coupled to the SPP Bloch modes. Satisfying the symmetry conditions, some of these Bloch states are optically active and can be coupled to photons. This is achieved when light of suitable polarization is incident upon the crystal under certain combinations of incidence angles and wavelengths, exchanging energy with plasmonic modes when diffraction from the periodic structure provides the wavevector conservation [9]:

$$\mathbf{k}_{\mathrm{SP}} = \frac{\omega}{c}\sin\theta\mathbf{u}_{xy}\delta_{s-p} \pm p\frac{2\pi}{D}\mathbf{u}_x \pm q\frac{2\pi}{D}\mathbf{u}_y\,, \qquad (1)$$

where $\delta_{s-p} = 1$ for p-polarized incident light (defined with respect to the film interface) and 0 for s-polarized light, $\mathbf{k}_{\mathrm{SP}}$ is the wave vector of the Bloch modes, $\mathbf{u}_{xy}$ is the unit vector in the direction of the in-plane component of the incident light wave vector, $\mathbf{u}_x$ and $\mathbf{u}_y$ are the unit reciprocal lattice vectors of a periodic structure, D is its periodicity (assumed to be the same in both x- and y-directions), and p and q are integer numbers corresponding to the different directions in the Brillouin zone. Since an SPP is in general a longitudinal excitation, the excitation light should have an electric field component perpendicular to the surface or parallel to the SPP propagation direction in order to be coupled to SPP waves.

An example of the zero-order normal incidence transmission spectra of two SPP crystals is shown in Fig. 1. The transmission spectrum of the bare (not coated with nonlinear polymer) crystal consists of a set of peaks corresponding to resonances in its spectrum of the electromagnetic modes that are coupled to photons. As a consequence of the polymer coating, both SPP Bloch modes and localized plasmon modes of the holes are significantly modified due to the changed dielectric constant of the hole filling and interface-adjacent medium from $n = 1$ (air) to $n \approx 1.7$ (nonlinear polymer). The observed changes in the transmission spectrum resulting from the polymer coating reflect the modification of the dispersion of the crystal and can be modelled using Eq. (1). The analysis of the band-gap structure and SPP Bloch modes of the coated SPP crystal shows that the peaks at around 750 nm and 620 nm correspond to the excitation of SPP Bloch modes ($\Gamma - M$ and $\Gamma - X$ directions, respectively) on the polymer/metal interface. The origin of the peak at around 700 nm is related to the coupling of localized surface plasmon resonances of the holes with SPP Bloch modes at the metal-polymer interface.

Taking advantage of the nonlinear response of the polymer, a control illumination can be used to modify its refractive index and, thus, the SPP modes and the associated

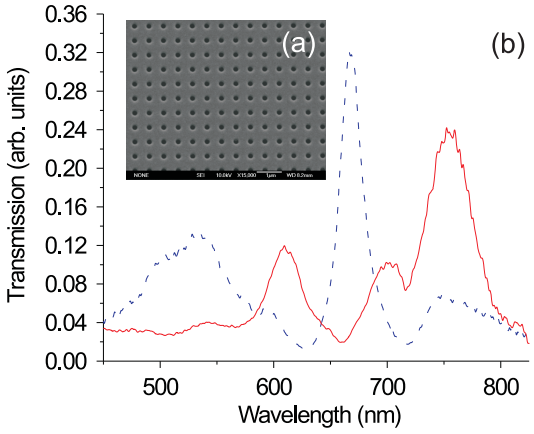

Figure 1 (online color at: www.lpr-journal.org) (a) SEM image of the nanostructured metal film used as a SPP crystal: Au film thickness-220 nm, hole diameter-200 nm, period-600 nm. (b) Normal incidence transmission spectra of the SPP crystal (dashed line) before and (solid line) after deposition of nonlinear polymer of about 200 nm thickness.

density of states of the nonlinear SPP crystal. These modifications then induce illumination-dependent changes in the optical transmission of the crystal. They can be monitored in the zero-order transmitted light spectrum as a function of the wavelength of a probe beam whose low intensity does not affect the polymer's permittivity (Fig. 2). The observed transmission changes are up to 60% of the initial transmittance of the SPP crystal in some transmission resonances (Fig. 2c). Nonlinear transmittance is observed at various wavelengths of the control light and demonstrate a similar behaviour in different spectral peaks exhibiting suppression (negative differential transmittance) or enhancement (positive differential transmittance) of the transmission. In addition to the changes in the transmission magnitude, the position of maxima and minima in the transmission spectra are also affected by the variation of the control intensity. This is an indication of the modification of the surface plasmon mode spectrum by the control light via induced changes in the polymer's dielectric constant.

Using the observed SPP band-gap shift, the changes in the effective refractive index of the polymer induced by the control light can be estimated to be $\Delta n \approx 10^{-3}$–10^{-4}. This estimation is based on a simple model considering an almost empty lattice and assuming uniform change of the polymer refractive index at the metal/polymer interface. In reality, however, the spatial variation of the induced refractive index changes follow the spatial variation of the field of the SPP modes excited by the control light and are significantly non-uniform. Therefore, larger local Δn values (greater than 10^{-3}) may be expected in the maxima of the field distributions at the control light wavelength. This is several orders of magnitude larger than the Δn changes detectable in sensing experiments with surface plasmons [31], thus, further reduction of the control light intensity may be possible.

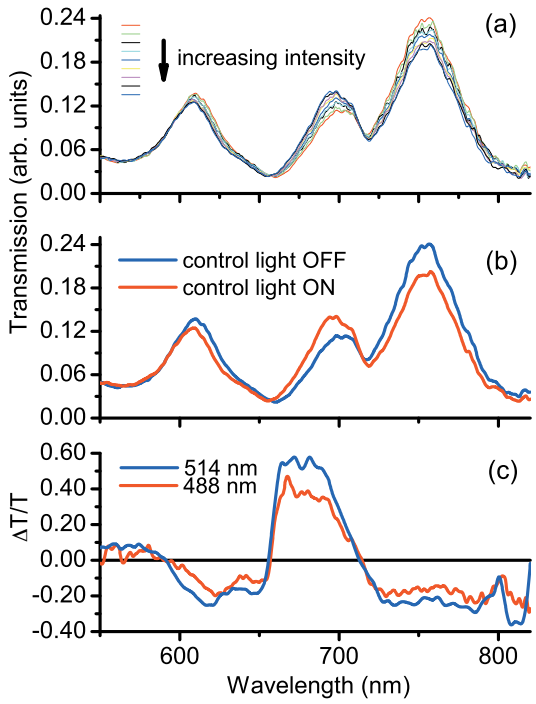

Figure 2 (online color at: www.lpr-journal.org) (a) Normal incidence transmission spectra of the hybridised SPP crystal illuminated with the 488 nm control light for the increasing illumination intensity. (b) Normal incidence transmission spectra of the nonlinear SPP crystal measured with the control light ($\lambda = 488$ nm, $P = 60$ mW) "on" and "off". (c) The induced differential transmittance spectra for the same intensity of the 488 nm and 514 nm control light as in (a).

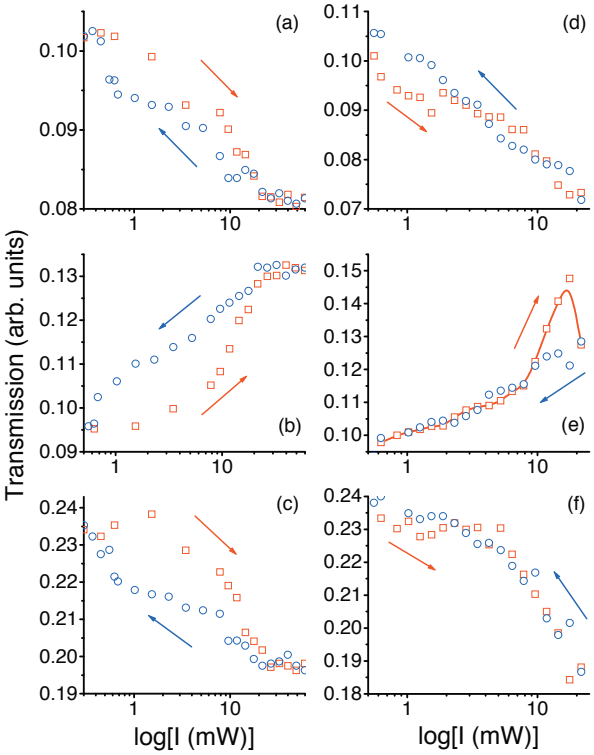

Figure 3 (online color at: www.lpr-journal.org) Dependence of the optical transmission of the nonlinear SPP crystal at (a,d) 620 nm, (b,e) 690 nm, and (c,f) 750 nm wavelengths for the increasing (squares) and decreasing (circles) control light intensity at (a–c) 488 nm and (d–f) 514 nm wavelengths.

3. Bistability of optical transmission through SPP crystals

For low intensity signal light, and neglecting the nonlinear response of the metal, the variations of the dielectric constant of the nonlinear material ε can be considered as solely induced by the control light of frequency ω_c:

$$\varepsilon(\mathbf{r},\omega) = \varepsilon^{(0)}(\omega) + 4\pi\chi^{(3)}|E_L(\varepsilon(\mathbf{r},\omega_c),\omega_c,\mathbf{r})|^2\,, \quad (2)$$

where $\varepsilon^{(0)}$ and $\chi^{(3)}$ are the linear dielectric constant and third-order nonlinear susceptibility of the polymer, respectively, and $E_L(\varepsilon(\mathbf{r}),\omega_c,\mathbf{r})$ is the local, position dependent ($\mathbf{r} = (x,y,z)$) electric field of the control light, which is determined by the SPP crystal parameters. Thus, the field distribution described by $E_L(\varepsilon(\mathbf{r}),\omega_c,\mathbf{r})$ depends on the induced permittivity changes in the nonlinear SPP crystal and, in turn, the permittivity variations depend on the local SPP field. As a consequence, the crystal's eigenmodes and associated field distribution for a given control intensity and wavelength self-consistently depend on the spatial variations of $\varepsilon(\mathbf{r})$. The permittivity variations modify the interaction of the signal light with the SPP crystal, thus, changing the transmission spectrum which is determined by the distribution of the dielectric constant around the nanostructured metal film [32, 33]. This leads to a multivalued dependence of the transmittance of SPP crystal on the control light intensity in the case of the dielectric constant dependence described by Eq.(2). The changes in the spatial distribution of the polymer's permittivity $\varepsilon(\mathbf{r})$ and the magnitude of these changes, both being responsible for the SPP crystal eigenmodes, provide a mechanism for bistable behaviour of the crystal's optical transmission with the intensity of the control light. As in a typical configuration for optical bistability, the above described process requires a nonlinear transmission dependence on the control light to achieve a transistor-type effect [1, 2] as well as a "built-in" feedback mechanism (described by Eq. (2)) to enable bistability [34, 35].

In the case of the SPP crystal considered in the previous section, for the control wavelength of 488 nm, and in the range of control intensities where only reversible changes of the transmission occur (below 5 kW/cm^2), bistability in the SPP crystal's transmission has been observed for all main resonances of the transmission spectrum (Fig. 3). However, the behaviour of the hysteresis loops with control intensity is different at different probe wavelengths: the transmission increases at some resonances and decreases at the others for the same variations of the control light

intensity. The complete switching occurs at similar control intensities for the transmission resonances considered, and the transmission returns to its original values when the control light is turned off.

The analysis shows that the different behaviour of the bistability loops observed at different probe wavelengths is related to the origin of the transmission resonances at these wavelengths. The peaks at around 750 nm and 620 nm exhibit a similar type of bistable behaviour and correspond to the excitation of SPP Bloch modes (in $\Gamma - M$ and $\Gamma - X$ directions, respectively) on the polymer/metal interface. For these wavelengths the influence of the nonlinearity is chiefly a modification of the absolute value of the transmittance at the resonance (Fig. 2. The behaviour of the peak at around 700 nm is more complicated: with an increased control intensity, not only does the transmittance change, but the peak shape changes. This highlights the complex origin of this peak corresponding to the coupling of localized surface plasmon resonances from the holes with SPP Bloch modes at the metal-polymer interface.

At the control wavelength of 514 nm (Fig. 3d–f), the nonlinear transmission is observed for all resonances as well. Compared to the experiments with the 488 nm control wavelength, the observed relative transmission changes in this case are up to 50% stronger at some signal wavelengths. However, the bistable effect is strongly present in the 690 nm resonance (the bistability is in this case observed at higher control intensities with an unusual "mini-loop" that may give some indication of two resonances involved [1, 3]), in other resonances the bistability is weak if any. The observed control wavelength dependence underlines the importance of both nonlinearity and feedback mechanism for the bistability to occur. At the 488 nm control wavelength, the nonlinear changes are smaller than at 514 nm but the feedback is stronger leading to bistability in the nonlinear transmission at all resonances of the SPP crystal. At the same time, in spite of the stronger nonlinear dependence of the transmission, bistability is not always present under the 514 nm control illumination due to a weaker feedback.

The dependence of the bistability type on the control light wavelength can be understood taking into account that the SPP field distribution at this wavelength plays a crucial role in triggering bistability. In particular, under the 488 nm and 514 nm illumination, different surface plasmon resonances of the metal-dielectric SPP crystal are excited (Fig. 1). Unfortunately, the near-field response corresponding to the different control light wavelengths cannot be experimentally estimated directly from the far-field transmission spectra. However, the analysis suggests that both the near-field intensity and its spatial distribution close to the metal-polymer interface, where nonlinear processes are most important, are responsible for the differences in nonlinear properties at the control wavelengths used.

This is illustrated by the numerical calculations of the electromagnetic field distributions in the SPP crystal hybridised with nonlinear polymer. The results are shown in Fig. 4. The field distributions above the metal/polymer interface are plotted for both 488 nm and 514 nm illumination wavelengths and show that a higher electric field intensity is generated between the holes in the case of the 488 nm control light wavelength (Fig. 4). Since the field around the hole is nearly identical, the SPP Bloch modes can be considered as the dominant origin of bistabilty. Despite the spectral position of the 488 nm control light above the surface plasmon resonance of the polymer-covered Au surface, it can excite the SPP modes if the polymer layer is thin enough [36]. In the case of 488 nm illumination, although the far-field transmission is smaller than at 514 nm wavelength, more energy is coupled to the SPP modes at the metal-dielectric interface. The changes in this coupling with the incident light intensity at the two wavelengths may explain the feedback difference in the two cases. Therefore, the different nonlinear behaviour triggered at 488 nm and 514 nm originates from the different spatial distributions and magnitude of the electromagnetic field at the metal-polymer interface. The modifications of the spatial variations of $\epsilon(\mathbf{r})$ and $E_L(\omega_c, \mathbf{r})$ are determined by the existing spatial distributions and values of these parameters in the moment of the intensity change occurs and, therefore, are different for the increasing and decreasing intensities of the control light.

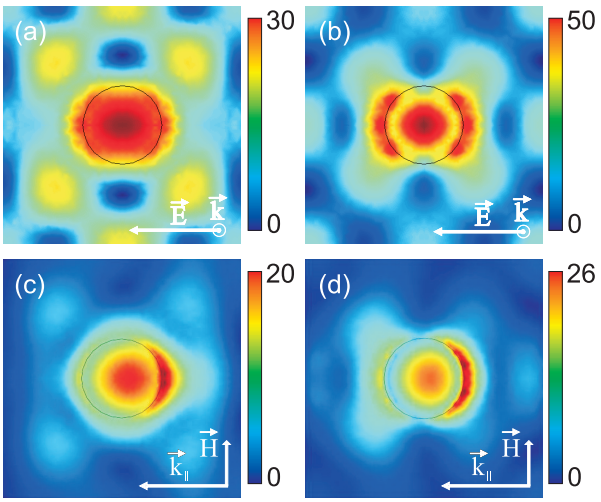

Figure 4 (online color at: www.lpr-journal.org) The control-light intensity distributions over a unit cell of the nonlinear SPP crystal as in Fig. 1 calculated using finite-element modelling at 10 nm distance above the metal surface on the nonlinear polymer side for (a,c) $\lambda = 488$ nm and (b,d) $\lambda = 514$ nm and the angle of incidence of (a,b) 0° and (c,d) 45°. $\mathbf{k}_{||}$ indicates the projection of the wave vector of the incident TM-polarized light.

Full numerical simulations of the nonlinear SPP crystals in various geometries have recently been performed using finite-different time domain modelling [29, 30]. Nonlinear SPP crystals have been modelled in the case of 1D structures (slit arrays) in a relatively thin metal films with nonlinear Kerr-materials in the slits as well as the overlayer of the metallic structure. In both cases the nonlinear transmission and its bistability was predicted due to the SPP

Bloch mode excitation in full agreement with the experiments in Ref. [26]. The earlier modelling of the gratings in a thick, perfect metal ($\mathrm{Re}\,\varepsilon = \infty$) with the slits filled with Kerr-type nonlinear dielectric also predicted bistability due to the waveguiding modes in the slits [37]. Bistability in transmission through the multilayered metal/dielectric structures due to the localized modes has also recently been shown [38]. Thus, various plasmonic and pure electromagnetic modes of metallic nanostructures hybritised with nonlinear materials can be used for triggering nonlinear response. Not only bistability effects but also beam shaping and manipulation [39, 40] as well as single photon optical nonlinearities can be achievable [17, 41, 42].

4. All-optical modulation of SPP crystal transmission

Building upon the nonlinear transmission of the hybridized SPP crystals and its dependence on the external light illumination, the all-optical modulation and gating of light with light can be realised. In order to achieve this effect at a very low control light intensity, one of the possibilities is to use smaller diameter of holes in the array similar to discussed above to increase the field confinement and, thus, enhancement. However, the drawback of this approach is a low intensity of the transmitted signal light through the SPP crystal.

The all-optical gating was demonstrated in an SPP crystal made of small (20 nm diameter) holes in thick (200 nm) Au film [25]. In this case, surface plasmon localization within the cylindrical channels leads to very strong field enhancements. As one can see from Fig. 5, the SPP crystal

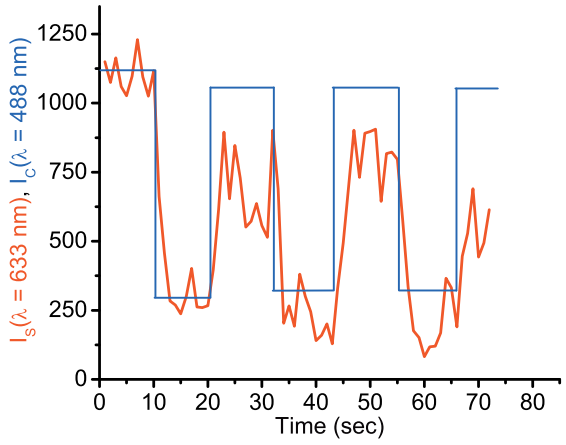

Figure 5 (online color at: www.lpr-journal.org) Modulation of the SPP crystal transmission at the 633 nm signal wavelength induced by the 488 nm control light. The control light was closed and opened three times during the experiment. The SPP crystal consists of 20 nm diameter holes in 400 nm free standing Au film arranged in 600 nm period square lattice. The intensity scales are internal for blue and red curves, not be compared.

transmission at the signal light wavelength ($\lambda = 633$ nm) is strongly affected by simultaneous illumination with control light ($\lambda = 488$ nm). In order to observe all-optical gating directly, the control light was modulated leading to the modulation of the transmission of SPP crystal. At the same time, for the SPP crystals in the similar configuration but with larger holes (~ 100 nm diameter), no significant variations of the transmission was observed for the same wavelengths and intensities of the signal and control light.

The time-response of the pure optical effects in such gating experiments is determined by the relaxation time of the excitons responsible for the Kerr nonlinearity in a polymer and the surface plasmon lifetime. The latter is on the scale of a few tens of femtoseconds and is much shorter than the response time of the nonlinear polymer which is in this case of about 10 ps [5]. Thus, very fast modulation and switching can be achieved in nonlinear SPP crystals with the speed limited by the nonlinear characteristics of nonlinear materials suitable for hybridization. It should be noted that in Fig. 5 the temporal behaviour of the modulation is determined by the time constant of the measurements (~ 3 s) needed for the optical transmission measurements through the hole array.

The investigation of the switching behaviour on the polarisation of the signal and control light provides an insight on nonlinear optical mixing processes in the nanoholes filled with nonlinear material. In the absence of the control light, transmission of p-polarized signal light is higher than the transmission of s-polarized light by approximately a factor of 3. This observation is consistent with the theoretical model of the enhanced transmission of SPP crystals relying on the excitation of surface polaritons on both film interfaces since at the oblique incidence the light of different polarizations interacts with different SPP resonances. This ratio of p- to s-polarized signal light transmission has been observed to be rather insensitive to the hole diameter in the studied range of the hole sizes. This should be expected since the spectrum of the SPP Bloch waves depends mainly on the periodicity of the structure. However, under the modulation with p-polarized control light, the p-to-s ratio in the signal light transmission is higher by approximately a factor of 20. Polarization measurements offer the best way to distinguish between nonlinear optical effects and possible thermal effects such as thermal expansion of the cylindrical channels, heating of the nonlinear material *etc.* that could interfere with the nonlinearity. Indeed, thermal modulation of the SPP crystal transmission can be observed at much larger (approximately by the factor of 1000) control light intensities. However, the polarization dependence of the signal light obtained under such conditions is very weak (Fig. 6c): the p-to-s ratio is only about 1.5.

The observed strong polarization dependence of the signal light modulation can be explained taking into account the properties of surface polariton Bloch waves on the periodically structured interfaces, the properties of surface plasmons in cylindrical channels, and the properties of the nonlinear susceptibility tensor $\chi^{(3)}$ of the nonlinear material. In the optical gating experiments, the SPP

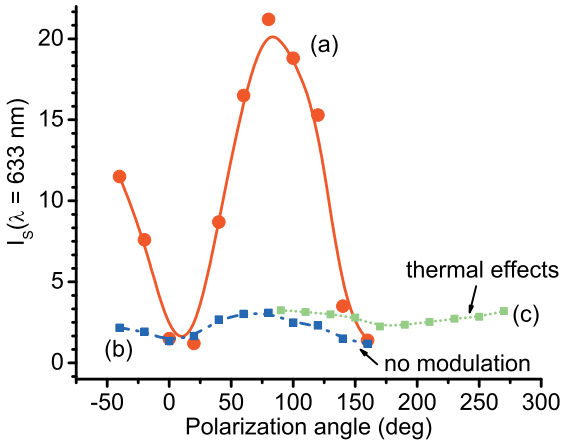

Figure 6 (online color at: www.lpr-journal.org) (a) Polarization dependence of the signal light modulation induced by the p-polarized control light. (b) Polarization dependence of the SPP crystal transmission at the signal wavelength in the absence of the control light. (c) Polarization dependence of the thermal modulation of the signal light which was observed at high control light intensity.

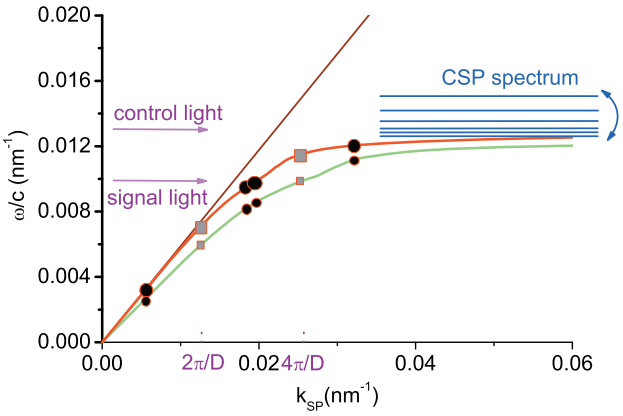

Figure 7 (online color at: www.lpr-journal.org) The SPP mode spectra of the SPPC embedded in the polymer. Schematic of the cylindrical surface plasmon (CSP) states in the polymer-filled channels at large wave vectors. (squares) SPP resonances excited with p-polarized light and (circles) SPP resonances excited with s-polarized light at the angle of incidence of 45°, light is incident along the hole rows. Positions of the signal and control light frequencies are shown by the arrows.

crystal was illuminated at an angle of incidence of approximately 45° so that the projection of the light wavevector onto the surface is in the direction corresponding to the direction along the hole rows ($\Gamma - X$ direction of the Brillouin zone). Therefore, according to Eq. (1), SPPs excited with s-polarised light correspond to the Bloch waves at the centre of the Brillouin zone (standing modes), while for p-polarized light they are propagating SPP Bloch waves far from the centre of the Brillouin zone.

The metal film under consideration is sufficiently thick to neglect the interaction between surface polaritons excited on different interfaces, therefore two independent sets of resonances can be considered [9]. The estimation of the positions of the band gaps in the SPP crystal can be performed using the approximation of an almost empty lattice which is appropriate for small diameter holes forming the SPP crystal (Fig. 7). Considering $\Gamma - X$ direction of the Brillouin zone, for p-polarised incident light and the angle of incidence of 45° used in the experiment, the SPP Bloch waves corresponding to 3rd and 4th Brillouin zone are excited at the wavelengths close to $\lambda = 633$ nm on the polymer-metal interface. At the same time for s-polarised light, the resonant SPP frequencies on the metal-polymer interface are far away from the signal light frequency. To complete the picture, the resonances associated with cylindrical channels in a metal film should be considered [43]. For thick films with well defined cylindricity of the channels ($d \ll h$), the spectrum of surface electromagnetic excitations in channels has a rather complicated structure with both radiative and nonradiative modes present. Individual cylindrical channels will have a discrete spectrum of resonances asymptotically approaching surface plasmon frequency ($\epsilon_m = -\epsilon$) from the high frequency side. For polymer-filled channels these modes overlap the frequency of the control blue light for large quantum numbers $s \gg 1$. The interaction between channels in an array can additionally broaden these resonances leading to minibands [44]. Thus, quasi-continuous spectrum of the states related to the cylindrical surface plasmons can be expected in the spectral range of the control light. For infinitely long cylindrical channels, the spectrum of wave vectors along the cylinder axis h_z is continuous, but is quantized due to Fabry-Perot-type resonances in the case of finite thickness film. From the physical point of view, one can imagine these excitations as surface modes of a spiral trajectory on a cylinder channel surface. Real (nonradiative) surface modes can not be excited directly by light, but at the frequency corresponding to the control light, the long-wavevector SPP can be excited on periodically perforated polymer-metal interface, which then can be coupled to cylindrical surface plasmons.

In the absence of control light, the signal light is transmitted via resonant tunneling through the states of SPP Bloch waves on the polymer-metal interface. Being confined to the polymer-coated interface, the SPP modes responsible for this transmission are very sensitive to the dielectric constant of the polymer, since changes of the dielectric constant modify the SPP resonant conditions and the transmission coefficient. Control light coupled into cylindrical surface plasmons results in the local changes of the dielectric constant of the polymer due to third-order Kerr nonlinearity. Local electromagnetic field is strongly enhanced in and around the channel due to cylindrical surface plasmon excitation because of the small volume of these surface modes ($E_L \sim 1/d$).

The polarization properties of the polymer molecules themselves play a significant role in the observed increase of the p-to-s ratio of the modulated signal light. The third-order nonlinearity of the polymer (3BCMU polydiacety-

lene) is contributed mainly by the π-electrons in the backbone of the polymer [45]. Each straight segment of polymer backbone could be treated as identical one-dimensional rod-like chromophore. At the microscopic level the $\chi^{(3)}$ tensor of the polymer is dominated by only one component: $\chi^{(3)}_{ssss}$, where s is the direction of the polymer chain. The preferential direction for the long polymer backbones inside narrow cylindrical channels forming the SPP crystal ought to be the direction along the channel. The nonlinear optical mixing is then determined by the components $D_l(\omega_0)$ of the optical field inside the channels at the signal wavelength:

$$D_l(\omega_0) = \chi^{(3)}_{ijkl} E_i(\omega_c) E_j(\omega_c) E_k(\omega_0)\,, \qquad (3)$$

where ω_c and ω_0 are the frequencies of the control and signal light, respectively. If the zzzz-components (along the channel direction) of $\chi^{(3)}_{ijkl}$ dominate the third-order susceptibility, the modulated signal light must be strongly p-polarized. At the same time, at the frequency of the control light ω_c, the electromagnetic field in the cylindrical channels is dominated by the plasmonic modes with large wave vectors along the channel, for which optical field oscillations have significant longitudinal component along the channel direction. Thus, one should expect the enhanced nonlinear optical mixing to occur while the electromagnetic field is propagating through small cylindrical holes.

5. Controlling optical transmission through individual apertures in SPP crystals

Having previously discussed the mechanisms of the optical transmission enhancement through SPP crystals, we can understand the optical properties of a single aperture surrounded by a periodic surface structure, which is important for applications in microscopy, optical and magneto-optical data storage, and photolithography. The aperture acts as a defect in a SPP crystal through which the energy of surface polaritons excited by the aperture surroundings is channelled, leading to significant enhancement of the field and enhancing the transmission through a metal film at its location. It would be advantageous to control the transmission of such an aperture all-optically using nonlinear effects.

One of the realisations of the high-throughput optical apertures is possible in multilayered metal films [46]. The optical transmission of an individual subwavelength aperture in an appropriately designed multilayered structure was shown to be enhanced compared to a homogeneous metal film. The enhancement effect is due to the light coupling to surface plasmon excitation which is facilitated by a film periodicity. The transmission enhancement in such a system also depends on the dielectric filling of the aperture. The latter effect can be used to switch and control the transmittance.

We will consider an example of a periodic multilayered structure (Fig. 8a) consisting of alternating layers of Au (thickness d_1) and Ag (thickness d_2) on a thick, free

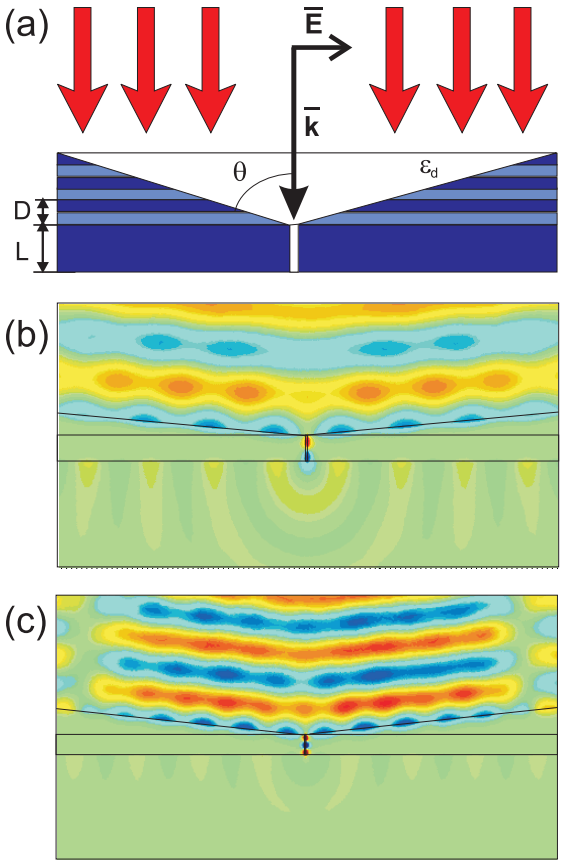

Figure 8 (online color at: www.lpr-journal.org) (a) Geometry of the mutilayered SPP crystal (not to scale with (b,c)): Au membrane thickness L, Au and Ag layers thickness d_1 and d_2, respectively, $D = d_1 + d_2$, cone opening angle θ, the aperture size is a. (b,c) The H_z component of the electromagnetic field distributions for light transmission through the aperture in the layered structure (b) in air (parameters of the structure $D = 46$ nm, $L = 200$ nm, $\theta = 86°$, $a = \lambda/50$) and (c) in the case when the aperture and the cone are filled with the dielectric $n = 1.5$ (parameters of the structure $D = 37$ nm, $L = 160$ nm, $\theta = 85°$, $a = \lambda/60$). H-field of the illuminating light ($\lambda = 633$ nm) is perpendicular to the image plane. The colour scales are internal for each image.

standing Au membrane (thickness L). The aperture of size a is made in the membrane while a conical depression centred at the aperture is made in the multilayered film. The periodicity of the multilayers and the opening angle of the aperture should be optimised to provide the resonant coupling conditions of light to SPPs at the given frequency of the incident light:

$$k_{\mathrm{SP}} = \frac{\omega}{c}\varepsilon_0^{1/2}\cos\theta + \frac{2\pi}{(d_1+d_2)}m\cos\theta\,, \qquad (4)$$

where k_{SP} is the wavevector of surface polaritons on the periodic structure (SPP Bloch waves), ω/c is the incident light wavevector, ε_0 is the dielectric constant of the filling of the conical depression, θ is the opening angle of the cone,

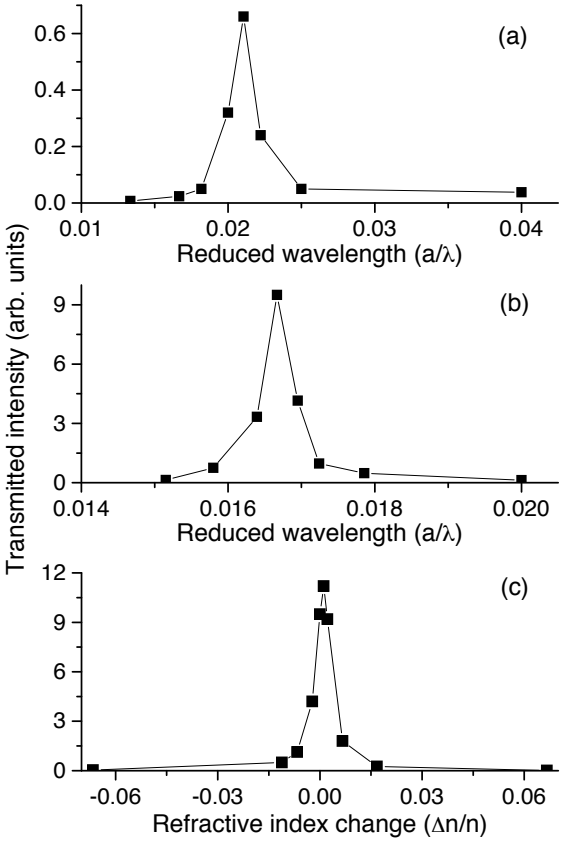

Figure 9 (a,b) The dependence of the transmitted intensity through the aperture in the layered structures presented in Figs. 8b and c, respectively, on the reduced wavelength. (c) The dependence of the transmitted intensity through the aperture on the refractive index changes of the dielectric filling in the aperture.

and m is the diffraction order. The light beam is assumed to be incident at the normal to the membrane (Fig. 8a).

The field distributions of light transmitted through the SPP crystal are shown in Fig. 8. The parameters of the Au/Ag nanostructure were designed to achieve the resonant transmission at the 633 nm wavelength ($\mathrm{Re}\,\varepsilon_{\mathrm{Au}} = -10$, $\mathrm{Re}\,\varepsilon_{\mathrm{Ag}} = -17$). In the case of the device operated in air (Fig. 8b), the cone opening was $\theta = 86°$ and periodicity $D = 45$ nm. The free standing Au membrane thickness was $L = 200$ nm, and the aperture size corresponds to $\lambda/50$. The periodic structure exhibits significantly enhanced transmission (by about 100 times in intensity) compared to the unstructured device or the device with geometrical parameters that do not correspond to the resonant conditions (Fig. 9a). These resonant conditions are highly sensitive and provide good wavelength discrimination in the transmitted light. The regions where SPP waves exist can be clearly distinguished due to shorter SPP wavelength (compared to the incident light) and respective interference patterns. The transmitted light intensity is strongest at the exit of the aperture and falls down with the distance from the surface due to spreading of the beam. The SPP excitation on the output facet of the device results in the delocalisation of the transmitted energy: the SPP waves are clearly observed on the Au surface (Fig. 8b,c).

If the cone is filled with nonlinear dielectric material the resonant conditions given by Eq. (4) are modified due to the different k_{SP} wavevector on the metal/dielectric interface but the transmission enhancement through the aperture can still be achieved at appropriate parameters of the structure (Figs. 8c and 9b). If variations in the refractive index of the nonlinear material are induced with an additional control beam illumination, the SPP coupling is modified leading to the changes of the transmitted intensity (Fig. 9c). This switching can be observed for both the modifications in the refractive index of the cone filling as well as only the aperture filling. In the latter case, this is due to the changes of Fabry-Perot SPP resonances in the aperture and/or modification of the SPP mode coupling into the aperture. Such a strong sensitivity to the filling can be used for controlling the transmission of the nanoscale holes as well as for sensing of molecules located in nanosized apertures.

6. Conclusion

We have presented a short overview of the physical principles and optical properties of nonlinear surface plasmon polaritonic crystals consisting of periodic plasmonic nanostructures hybridised with nonlinear dielectric. Owing to the field enhancement effects and high sensitivity of SPP Bloch modes to the permittivity of the adjacent dielectric, SPPCs provide a straightforward route to realising nonlinear photonic devices operating at very low control light intensities. The size of these plasmonic components is small enough to be easily integrated into photonic and optoelectronic chips.

We have shown that the nonlinear optical transmission through hybridised surface plasmon polaritonic crystals exhibits optical bistability with varying control light intensity. The effect is relying on the modification of the SPP Bloch mode spectrum of the SPPC due to the nonlinearity of the adjacent polymer. The nonlinear transmission of SPP crystals can be also observed by addressing the resonances of cylindrical surface plasmons for the control light enhancement. Cylindrical surface plasmons provide stronger field enhancement and, therefore, lower control light intensities. The approach based on the SPP Bloch modes allows generally lower field enhancement than cylindrical surface plasmons but provides more flexibility for optimising the spectral response of the structure and higher signal throughput. It should be noted that the bistability observed in transmission through SPP crystals is a consequence of the bistability of SPP Bloch modes and, thus, SPP waves propagating on the metal interface. Therefore, nonlinear (including bistable) behaviour of SPP waves guided through the SPP crystal is also expected.

The functionalities available with nonlinear SPP crystals include all-optical modulation and switching as well as optical transistor effects relying on coupling of the photons to plasmonic excitations followed by the increased

nonlinear interaction between plasmonic states as well as on in-plane guided SPP waves. The high sensitivity to the dielectric surroundings, including the aperture filling in the case of ideal SPPCs [47] as well as SPPC defects can be used in chemo- and bio-sensing of entities present in the apertures. Tuneable spectral filters for harsh environments and in space-based applications is another possible application.

Acknowledgements This work was supported, in part, by EPSRC (UK) and EU FP6 Network of Excellence Plasmo-Nano-Devices. The authors are grateful to W. Dickson, R. Pollard, J. Elliott, C. C. Davis, I. I. Smolyaninov, and A. Stanishevsky for fruitful collaboration on the subject of the review.

Gregory Wurtz received his PhD in Physics from the University of Troyes, France in 2000. His dissertation was on near-field optical microscopy. He then pursued work in nano-optics in several institutions in the USA, France and the UK from 2000 to 2007 when he joined the University of North Florida as an Assistant Professor of Physics. His present research interests include the use of time resolved optical spectroscopies and spatially resolved scanning probe microscopies to study hybrid nanostructured plasmonic materials for the design of nanodevices.

Professor Anatoly V. Zayats is a head of the Nano-optics and Near-field Spectroscopy group in the Centre for Nanostructured Media, The Queen's University of Belfast.

He graduated and received PhD degree in physics from Moscow Institute of Physics and Technology (USSR) in 1986 and 1989, respectively. In 1999 he joined The Queen's University of Belfast. His current research interests are in the areas of near-field optics, scanning probe microscopy, nanophotonics and plasmonics, nonlinear optics and spectroscopy, surface plasmons and polaritons, and optical properties of surfaces, thin films, semiconductors and low-dimensional structures. He is a Fellow of Institute of Physics and Optical Society of America.

References

[1] H. M. Gibbs, Optical Bistability: Controlling Light with Light (Academic, New York, 1985).
[2] S. John and M. Florescu, J. Opt. A, Pure Appl. Opt. **3**, S103-S120 (2001).
[3] R. A. Innes and J. R. Sambles, J. Phys. Condens. Matter **1**, 6231–6260 (1989).
[4] W. Dickson, G. A. Wurtz, P. R. Evans, R. J. Pollard, and A. V. Zayats, Nano Lett. **8**, 281–286 (2008).
[5] D. S. Chemla and J. Zyss (Eds.), Nonlinear Optical Properties of Organic Molecules and Crystals, (Academic, New York, 1987).
[6] E. Centeno and D. Felbacq, Phys. Rev. B **62**, R7683–R7686 (2000).
[7] S. F. Mingaleev and Yu. S. Kivshar, J. Opt. Soc. Am. B **19**, 2241–2249 (2002).
[8] M. F. Yanik, S. Fan, M. Soljacic, and J. D. Joannopoulos, Opt. Lett. **28**, 2506–2508 (2003).
[9] A. V. Zayats, I. I. Smolyaninov, and A. A. Maradudin, Phys. Rep. **408**, 131–314 (2005).
[10] S. A. Maier, Plasmonics: Fundamentals and Applications (Springer, New York, 2007).
[11] I. I. Smolyaninov, Phys. Rev. Lett. **94**, 057403 (2005).
[12] T.-M. Liu, S.-P. Tai, C.-H. Yu, Y.-C. Wen, S.-W. Chu, L.-J. Chen, M. R. Prasad, K.-J. Lin, and C.-K. Sun, Appl. Phys. Lett. **89**, 043122 (2006).
[13] Y. Shen and P. N. Prasad, Appl. Phys. B **74**, 641–645 (2002).
[14] M. A. Noginov, G. Zhu, V. P. Drachev, and V. M. Shalaev, in: Nanophotonics with Surface Plasmons, edited by V. M. Shalaev and S. Kawata (Elsevier, Amsterdam, 2007), pp. 141–169.
[15] W. Dickson, P. Evans, G. A. Wurtz, W. Hendren, R. Atkinson, R. J. Pollard, and A. V. Zayats, J. Microsc. **229**, 415–420 (2008).
[16] D. C. Marinica, A. G. Borisov, and S. V. Shabanov, Phys. Rev. B **76**, 085311 (2006).
[17] I. I. Smolyaninov, A. V. Zayats, A. Gungor, and C. C. Davis, Phys. Rev. Lett. **88**, 187402 (2002).
[18] I. I. Smolyaninov, C. C. Davis, and A. V. Zayats, Appl. Phys. Lett. **81**, 3314–3316 (2002).
[19] W. L. Barnes, A. Dereux, and T. W. Ebbesen, Nature **424**, 824–830 (2003).
[20] L. Salomon, F. Grillot, A. V. Zayats, and F. de Fornel, Phys. Rev. Lett. **86**, 1110–1113 (2001).
[21] N. E. Glass and A. A. Maradudin, Phys. Rev. B **29**, 1840–1847 (1984).
[22] W. L. Barnes, T. W. Preist, S. C. Kitson, and J. R. Sambles, Phys. Rev. B **54**, 6227–6244 (1996).
[23] M. Kretschmann and A. A. Maradudin, Phys. Rev. B **66**, 245408 (2002).
[24] H. Raether, Surface Plasmons (Springer, Berlin, 1988).
[25] I. I. Smolyaninov, A. V. Zayats, A. Stanishevsky, and C. C. Davis, Phys. Rev. B **66**, 205414 (2002).
[26] G. A. Wurtz, R. Pollard, and A. V. Zayats, Phys. Rev. Lett. **97**, 057402 (2006).
[27] A. M. Dykhne, A. K. Sarychev, and V. M. Shalaev, Phys. Rev. B **67**, 195402 (2003).
[28] J. A. van Nieuwstadt, M. Sandtke, R. H. Harmsen, F. B. Segerink, J. C. Prangsma, S. Enoch, and L. Kuipers, Phys. Rev. Lett. **97**, 146102 (2006).
[29] C. Min, P. Wang, X. Jiao, and H. Min, Opt. Express **15**, 12368–12373 (2007).
[30] C. Min, P. Wang, C. Chen, Y. Deng, H. Min, T. Ning, Y. Zhou, and G. Yang, Opt. Lett. **33**, 900–902 (2008).
[31] P. N. Prasad, Introduction to Biophotonics (Wiley, New York, 2003).

[32] S. A. Darmanyan and A. V. Zayats, Phys. Rev. B **67**, 035424 (2003).
[33] S. A. Darmanyan, M. Nevière, and A. V. Zayats, Phys. Rev. B **70**, 075103 (2004).
[34] E. Garmire, IEEE J. Quantum Electron. **25**, 289–295 (1989).
[35] D. A. B. Miller, A. C. Gossard, and W. Wiegmann, Opt. Lett. **9**, 162–164 (1984).
[36] A. Karalis, E. Lidorikis, M. Ibanescu, J. D. Joannopoulos, and M. Soljacic, Phys. Rev. Lett. **95**, 063901 (2005).
[37] J. A. Porto, L. Martín-Moreno, and F. J. García-Vidal, Phys. Rev. B **70**, 081402 (2004).
[38] A. Husakou and J. Hermann, Phys. Rev. Lett. **99**, 127402 (2007).
[39] C. Min, P. Wang, X. Jiao, and H. Min, Opt. Express **15**, 9541–9546 (2007).
[40] C. Min, P. Wang, X. Jiao, and H. Min, Appl. Phys. B **90**, 97–99 (2008).
[41] K. M. Birnbaum, A. Boca, R. Miller, A. D. Boozer, T. E. Northup, and H. J. Kimble, Nature **436**, 87–90 (2005).
[42] D. E. Chang, A. S. Sorensen, E. A. Demler, and M. D. Lukin, Nature Physics **3**, 807–812 (2007).
[43] A. D. Boardman (Ed.), Electromagnetic Surface Modes, (Wiley, New York, 1982).
[44] V. Kuzmiak, A. A. Maradudin, and F. Pincemin, Phys. Rev. B **50**, 16835–16844 (1994).
[45] K. Yang, W. Kim, A. Jain, J. Kumar, and S. Tripathy, Optics Commun. **164**, 203–210 (1999).
[46] A. V. Zayats and I. I. Smolyaninov, Opt. Lett. **31**, 398–400 (2006).
[47] J. M. McMahon, J. Henzie, T. W. Odom, G. C. Schatz, and S. K. Gray, Opt. Express **15**, 18119–18129 (2007).